The effect of disorder geometry on the critical force in disordered elastic systems

J. Stat. Mech. (2014) P03009

(http://iopscience.iop.org/1742-5468/2014/3/P03009)

Journal of Statistical Mechanics: Theory and Experiment
An IOP and SISSA journal

The effect of disorder geometry on the critical force in disordered elastic systems

Vincent Démery[1,2], **Vivien Lecomte**[3] **and Alberto Rosso**[4]

[1] Institut Jean Le Rond d'Alembert (UMR CNRS 7190), Université Pierre et Marie Curie, F-75005 Paris, France
[2] Department of Physics, University of Massachusetts, Amherst, MA 01003, USA
[3] Laboratoire Probabilités et Modèles Aléatoires (UMR CNRS 7599), Université Pierre et Marie Curie and Université Paris Diderot, F-75013 Paris, France
[4] Laboratoire Physique Théorique et Modèles Statistiques (UMR CNRS 8626), Université de Paris-Sud, Orsay Cedex, France
E-mail: vdemery@physics.umass.edu, vivien.lecomte@gmail.com and alberto.rosso@u-psud.fr

Received 2 December 2013
Accepted for publication 26 January 2014
Published 11 March 2014

Online at stacks.iop.org/JSTAT/2014/P03009
doi:10.1088/1742-5468/2014/03/P03009

Abstract. We address the effect of disorder geometry on the critical force in disordered elastic systems. We focus on the model system of a long-range elastic line driven in a random landscape. In the collective pinning regime, we compute the critical force perturbatively. Not only does our expression for the critical force confirm previous results on its scaling with respect to the microscopic disorder parameters, but it also provides its precise dependence on the disorder geometry (represented by the disorder two-point correlation function). Our results are successfully compared with the results of numerical simulations for random field and random bond disorders.

Keywords: classical phase transitions (theory), interfaces in random media (theory), disordered systems (theory), heterogeneous materials (theory)

1742-5468/14/P03009+20$33.00

Contents

1. Introduction

Disordered elastic systems [1]–[4] are ubiquitous in Nature and condensed matter physics; they encompass a wide range of systems going from vortex lattices in superconductors [5] to ferromagnetic domain walls [6], wetting fronts [7], imbibition fronts [8, 9] or crack fronts in brittle solids [10, 11]. In simple models for these phenomena, an elastic object struggles to stay flat while its random environment tries to deform it, in or out of equilibrium. An example is given by an elastic line in a random landscape, which is pictured in figure 1. As a result of the competition between disorder and elasticity, the elastic object becomes rough and is characterized by a universal roughness exponent [12, 13] that depends on the dimension of the problem, the range of the elastic interaction and the type of disorder, but not on the microscopic details of the system [2, 4].

This coupling between disorder and elasticity also has an important consequence on the response of the elastic object to an external force [5]. At zero temperature, there exists a critical force below which it does not move and remains *pinned* by the disorder. If the applied force is larger than this threshold, the elastic object *unpins* and acquires a non-zero average velocity. This describes the *depinning transition* of the elastic line. A finite temperature rounds this behaviour for forces close to the threshold [14] and

J. Stat. Mech. (2014) P03009

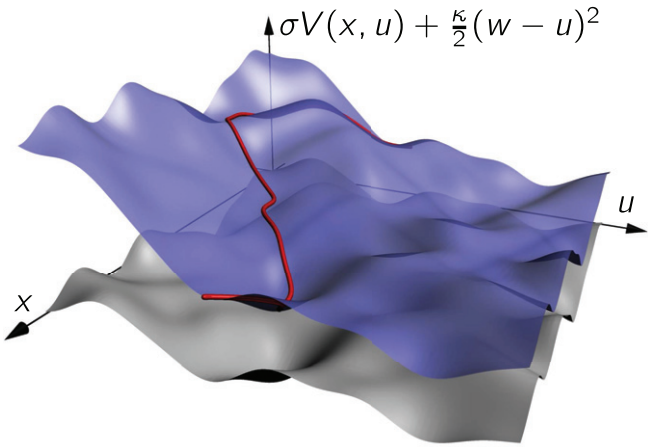

Figure 1. An elastic line pulled by a spring of stiffness κ and position w in a random landscape. The bottom grey surface is the potential $\sigma V(x,u)$. The top blue surface is the effective potential seen by the line, i.e. the bare potential plus the parabolic potential $\kappa(w-u)^2/2$ exerted by the spring.

allows the object to move at a finite velocity for forces well below the threshold, by a thermally activated motion called *creep* [15]–[19]. The critical force plays a crucial role in applications. In type-II superconductors, it corresponds to the critical current above which the vortex lattice starts moving, leading to a superconductivity breakdown [20]. In brittle solids, it determines the critical loading needed for a crack to propagate through the sample and break it apart [10].

In contrast to roughness and depinning exponents, the critical force is not a universal quantity and its value depends in general on the details of the model. Powerful techniques such as the functional renormalization group allow the determination of universal exponents [21]–[23], but one has to resort to other approaches for the critical force. Scaling arguments allow one to find its dependence on the disorder amplitude and the different length scales present in the system, such as the size of the defects and the typical distance between them [5, 24]. Unfortunately this approach gives the critical force only up to a numerical prefactor, whose value depends on microscopic quantities such as the geometrical shape of the impurities, and which is essential to determine in view of applications. Recently, a numerical self-consistent scheme [25, 26] and numerical simulations have focused on a precise determination of the critical force [27, 28] in the context of brittle failure. Notably, is has been shown that in the *collective* regime, occurring at weak disorder amplitude, the critical force does not depend on the disorder distribution but only on the disorder amplitude and correlation length [27]. Still, the effect of the disorder geometry, which is partly encoded in its two-point correlation function, remains to be determined.

In this paper, we address the question of the dependence of the critical force on the disorder geometry. We focus on the case of a long-range elastic line in a random potential, which is the relevant model for wetting fronts and crack fronts in brittle failure. We restrict ourselves to the collective pinning regime, which appears when the disorder amplitude is

J. Stat. Mech. (2014) P03009

small. The line is driven by a spring pulled at constant velocity, and the *drag force* needed to move the spring is computed perturbatively in the disorder amplitude. In the limit of zero spring stiffness and zero velocity, this force is the critical force and we derive its analytic expression.

Our expression depends explicitly on the two-point correlation function of the disorder, and thus on the disorder geometry. Moreover, our computation is valid for a random bond disorder as well as a random field disorder [18]. Numerical simulations are performed for both types of disorder and various disorder geometries. They provide a successful check of our analytical result and show that two systems with the same disorder amplitude and correlation length can have different critical forces if their disorder two-point correlation functions are different.

The paper is organized as follows. In section 2, we introduce the model of a long-range elastic line driven in a random landscape. In section 3, we summarize our results. Section 4 is devoted to the analytical computation of the drag force, from which we deduce the critical force. Numerical simulation details and results are presented in section 5. We conclude in section 6.

2. Model

We consider a $1+1$ dimensional elastic line of internal coordinate x and position $u(x,t)$, pulled by a spring of stiffness κ located at position $w(t)$ in a random energy landscape $\sigma V(x,u)$; this system is represented in figure 1. The parameter σ represents the disorder amplitude. The equation of evolution of the line position at zero temperature is [2, 29]

$$\partial_t u(x,t) = \kappa[w(t) - u(x,t)] + f_{\mathrm{el}}[u(\cdot,t)](x) - \sigma\partial_u V(x,u(x,t)). \tag{1}$$

The elastic force $f_{\mathrm{el}}[u(\cdot,t)](x)$ is linear in $u(x,t)$ and we consider the case of a long-range elasticity

$$f_{\mathrm{el}}[u(\cdot,t)](x) = \frac{c}{\pi}\int \frac{u(x',t)-u(x,t)}{(x-x')^2}\,\mathrm{d}x'. \tag{2}$$

The disorder has zero mean ($\overline{V(x,u)} = 0$) and two-point correlation function

$$\overline{V(x,u)V(x',u')} = R_x(x-x')R_u(u-u'). \tag{3}$$

The overline represents the average over the disorder. Alternatively, one can also use the force correlation function,

$$\overline{\partial_u V(x,u)\partial_{u'}V(x',u')} = -R_x(x-x')\partial_u^2 R_u(u-u') \tag{4}$$

$$= \Delta_x(x-x')\Delta_u(u-u'), \tag{5}$$

with $\Delta_u = -\partial_u^2 R_u$. We do not assume that the disorder is Gaussian distributed. For the so-called random bond (RB) case, the potential $V(x,u)$ is short-range correlated in both the variables x and u; this implies a global constraint on the force correlation function, namely $\int \Delta_u(u)\,\mathrm{d}u = 0$. For the random field (RF) case, $V(x,u)$ is, for instance, a Brownian motion as a function of u, with diffusion constant $\int \Delta_u(u)\,\mathrm{d}u > 0$ [18].

J. Stat. Mech. (2014) P03009

Finally, we impose a constant velocity v on the spring,

$$w(t) = vt. \tag{6}$$

The drag f_{dr} is defined to be the average force exerted on the line by the spring,

$$f_{\mathrm{dr}}(\kappa, v) = \kappa \left[w(t) - \overline{\langle u(x,t) \rangle} \right], \tag{7}$$

where $\langle \cdot \rangle$ denotes the average along the internal coordinate x. Since the landscape is statistically translation invariant, this quantity is expected to not depend on time. Besides, it is expected that both the drag force and the critical force, which depend on the realization of the disorder, will tend to a limit at large system size which is independent of the particular realization—hence equal to its average over disorder, which we make use of in (7). These averages are the so-called *thermodynamic* drag and critical forces.

We focus on the computation of the drag as a function of the spring stiffness κ and velocity v. We then show how to extract the critical force from these force–velocity characteristics, fixing the velocity instead of the force.

3. Main result

Our main result is the following expression for the critical force, valid in the collective pinning regime (when the disorder amplitude σ is small):

$$f_{\mathrm{c}} \simeq \frac{\sigma^2 \tilde{\Delta}_x(0)}{4\pi c} \int |k_u| \tilde{\Delta}_u(k_u)\, \mathrm{d}k_u, \tag{8}$$

where $\tilde{\Delta}_{x,u}$ are Fourier transforms of $\Delta_{x,u}$. The expression of f_{c} holds for a long-range elastic line for both random bond and random field disorders. It is compared to simulation results in figure 2, which shows a very good agreement in the collective pinning regime $\Sigma \ll 1$. The dimensionless disorder amplitude Σ is defined later (40).

This analytic result is derived in section 4 and the numerical simulations are detailed in section 5.

4. Analytical computation

In this section, we start by computing the average force required to drive the line at an average speed v with a spring of stiffness κ. This provides us with a force–velocity characteristic curve that depends on the spring stiffness. From these characteristic curves, we deduce that sending the velocity and stiffness to zero in the appropriate order allows us to extract the critical force.

4.1. Drag force

The line evolution equation (1) is highly non-linear due to the presence of the random potential; it is thus very difficult to handle. To evaluate the average drag, we resort to a perturbative analysis in the disorder amplitude σ.

J. Stat. Mech. (2014) P03009

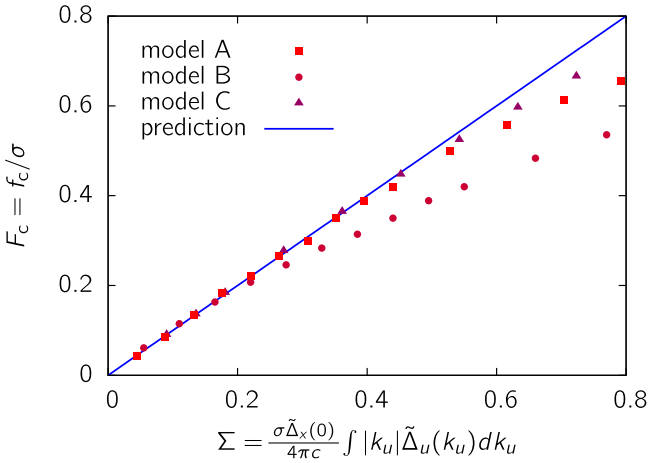

Figure 2. Critical force as a function of the dimensionless disorder amplitude Σ, defined in (40): comparison between numerical simulations and analytical prediction (8) for random field (models A and B) and random bond (model C) disorders (the disorders are defined precisely in section 5.1). The points are the results of the simulations and the line is the analytical prediction, valid in the small Σ limit.

We expand the line position in powers of σ as

$$u(t) = \sum_n \sigma^n u_n(t). \tag{9}$$

At order 0, the solution of (1) is independent of disorder,

$$u_0(x,t) = vt - \frac{v}{\kappa}, \tag{10}$$

leading from (7) to the average drag

$$f_{\mathrm{dr}}^{(0)}(\kappa, v) = v. \tag{11}$$

The computation at higher orders is carried out in Fourier space, with the convention $\tilde{g}(k_x) = \int g(x)\mathrm{e}^{-\mathrm{i}k_x x}\,\mathrm{d}x$ (and similarly along direction u). We start by Fourier transforming the elastic force,

$$f_{\mathrm{el}}[u(\cdot,t)](x) = -c\int |k_x|\tilde{u}(k_x,t)\mathrm{e}^{\mathrm{i}k_x x}\frac{\mathrm{d}k_x}{2\pi}, \tag{12}$$

and the disorder correlator,

$$\overline{\tilde{V}(k_x,k_u)\tilde{V}(k'_x,k'_u)} = (2\pi)^2\delta(k_x+k'_x)\delta(k_u+k'_u)\tilde{R}_x(k_x)\tilde{R}_u(k_u). \tag{13}$$

We also define, corresponding to (4) and (5),

$$\tilde{\Delta}_x(k_x) = \tilde{R}_x(k_x), \tag{14}$$
$$\tilde{\Delta}_u(k_u) = k_u^2\tilde{R}_u(k_u). \tag{15}$$

The first order contribution to the line position satisfies

$$\partial_t u_1(x,t) + \kappa u_1(x,t) - f_{\rm el}[u_1(\cdot,t)](x) = -\partial_u V(x,u_0(t)). \tag{16}$$

Fourier transforming this equation in directions x and u gives the solution in Fourier space,

$$\tilde{u}_1(k_x,t) = -\int \frac{{\rm i}k_u}{{\rm i}k_u v + \omega(k_x)} {\rm e}^{{\rm i}k_u u_0(t)} \tilde{V}(k_x,k_u) \frac{{\rm d}k_u}{2\pi}, \tag{17}$$

where we have introduced the damping rate

$$\omega(k_x) = \kappa + c|k_x|, \tag{18}$$

which fully encompasses the effect of the elasticity. Since the first order correction is linear in the potential V, its average over disorder is 0 and it does not contribute to the drag: $f_{\rm dr}^{(1)} = 0$.

At second order, the evolution equation reads

$$\partial_t u_2(x,t) + \kappa u_2(x,t) - f_{\rm el}[u_2(\cdot,t)](x) = -\sigma^{-1}[\partial_u V(x,u_0(t)+\sigma u_1(x,t)) - \partial_u V(x,u_0(t))]. \tag{19}$$

Following an idea introduced by Larkin [30], we expand the potential around $u_0(t)$, getting

$$\partial_t u_2(x,t) + \kappa u_2(x,t) - f_{\rm el}[u_2(\cdot,t)](x) = -\partial_u^2 V(x,u_0(t)) u_1(x,t). \tag{20}$$

It reads in Fourier space

$$\partial_t \tilde{u}_2(k_x,t) + \omega(k_x)\tilde{u}_2(k_x,t) = \int k_u^2 {\rm e}^{{\rm i}k_u u_0(t)} \tilde{V}(k'_x,k_u) \tilde{u}_1(k_x-k'_x,t) \frac{{\rm d}k'_x\,{\rm d}k_u}{(2\pi)^2}. \tag{21}$$

Inserting the first order result (17) and solving gives

$$\tilde{u}_2(k_x,t) = \int \frac{{\rm i}k_u'^2 (k'_u - k_u) {\rm e}^{{\rm i}k_u u_0(t)}}{[{\rm i}k_u v + \omega(k_x)][{\rm i}(k_u-k'_u)v + \omega(k_x-k'_x)]} \times \tilde{V}(k_x-k'_x,k_u-k'_u)\tilde{V}(k'_x,k'_u) \frac{{\rm d}k'_x\,{\rm d}k_u{\rm d}k'_u}{(2\pi)^3}. \tag{22}$$

Averaging over disorder with (13) leads to

$$\overline{\tilde{u}_2(k_x)} = 2\pi\delta(k_x) \int \frac{{\rm i}k_u \tilde{\Delta}_x(k'_x)\tilde{\Delta}_u(k_u)}{\kappa[-{\rm i}k_u v + \omega(k'_x)]} \frac{{\rm d}k'_x\,{\rm d}k_u}{(2\pi)^2}. \tag{23}$$

J. Stat. Mech. (2014) P03009

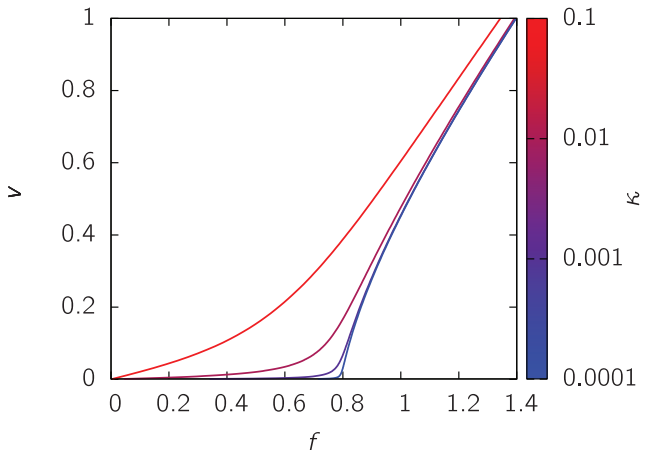

Figure 3. Force–velocity curve using the drag (27) computed to the second order in σ, for different values of the parabola curvature κ, indicated by the colour scale. The two-point functions Δ_x and Δ_u of the disorder are centred Gaussian functions of unit variance, encoding a random field disorder.

The proportionality to $\delta(k_x)$ signifies that, in direct space, the average second order correction does not depend on the internal coordinate x. It reads

$$\overline{u_2} = -\int \frac{v k_u^2 \tilde{\Delta}_x(k_x)\tilde{\Delta}_u(k_u)}{\kappa[k_u^2 v^2 + \omega(k_x)^2]} \frac{\mathrm{d}k_x\,\mathrm{d}k_u}{(2\pi)^2}. \tag{24}$$

The second order drag is thus

$$f_{\mathrm{dr}}^{(2)}(v,\kappa) = \sigma^2 \int \frac{v k_u^2 \tilde{\Delta}_x(k_x)\tilde{\Delta}_u(k_u)}{k_u^2 v^2 + (\kappa + c|k_x|)^2} \frac{\mathrm{d}k_x\,\mathrm{d}k_u}{(2\pi)^2}. \tag{25}$$

Adding this result to the zeroth order drag (11) provides the drag up to the order σ^2,

$$f_{\mathrm{dr},2}(v,\kappa) = f_{\mathrm{dr}}^{(0)}(v,\kappa) + f_{\mathrm{dr}}^{(1)}(v,\kappa) + f_{\mathrm{dr}}^{(2)}(v,\kappa) \tag{26}$$

$$= v + \sigma^2 \int \frac{v k_u^2 \tilde{\Delta}_x(k_x)\tilde{\Delta}_u(k_u)}{k_u^2 v^2 + (\kappa + c|k_x|)^2} \frac{\mathrm{d}k_x\,\mathrm{d}k_u}{(2\pi)^2}. \tag{27}$$

This drag gives us access, at the perturbative level, to the crucial force–velocity characteristic. It is plotted in figure 3 for a random field disorder with Gaussian two-point functions, at different values of the spring stiffness. When the spring stiffness κ goes to zero, the depinning transition appears clearly and becomes sharp when $\kappa = 0$. The picture is qualitatively similar for a random bond disorder. Any positive stiffness rounds the transition, analogously to the temperature [4, 14, 31].

4.2. Critical force

As noted above, the usual force–velocity characteristic at zero temperature is recovered in the limit $\kappa \to 0$; its equation is given by

$$f_{\kappa=0,2}(v) = v + \frac{\sigma^2}{c} \int \frac{k_u^2 \tilde{\Delta}_x(vq/c)\tilde{\Delta}_u(k_u)}{k_u^2 + q^2} \frac{\mathrm{d}q\,\mathrm{d}k_u}{(2\pi)^2}. \tag{28}$$

We have performed the variable substitution $ck_x = vq$ in order to eliminate the velocity in the denominator. Taking the small velocity limit in this expression gives the critical force (8)

$$f_{c,2} = \frac{\sigma^2 \tilde{\Delta}_x(0)}{4\pi c} \int |k_u| \tilde{\Delta}_u(k_u)\, \mathrm{d}k_u. \tag{29}$$

This expression is our main result, announced in equation (8). The index 2 indicates that this critical force comes from a second order perturbative computation in the disorder amplitude σ. The two limits do not commute: since any non-zero stiffness rounds the transition, taking the limit of zero velocity first would give a zero critical force (see figure 3). To get the depinning exponent β defined by $v \sim_{f \to f_c^+} (f - f_c)^\beta$, we have to go one step further in the Taylor expansion of (28) around $v = 0$. This can be done analytically for simple correlators $\tilde{\Delta}_x(k_x)$ and $\tilde{\Delta}_u(k_u)$, or numerically in the general case (see figure 3 for an example). We get

$$v \sim f - f_c, \tag{30}$$

which corresponds to the mean field behaviour $\beta = \beta_{MF} = 1$ [32] valid above the upper critical dimension d_{uc} (for the long-range elasticity $d_{uc} = 2$). Below d_{uc}, the mean field value $\beta_{MF} = 1$ is an upper bound of the exact value of β which can be estimated by a functional renormalization group ϵ-expansion [21]–[23] or evaluated numerically to $\beta = 0.625 \pm 0.0005$ for the long-range elastic line [33].

5. Numerical simulations

We now turn to the comparison of our analytical prediction with numerical simulations of the line. Since our computation remains valid for both random bond and random field disorder, we perform numerical simulations for both cases.

5.1. Numerical model

In our model a line of length L is discretized with a step a and its elasticity is given by

$$f_{el}[u(\cdot,t)]_n = \frac{c}{\pi a} \sum_{n' \neq 0} \frac{u_{n'}(t) - u_n(t)}{(n-n')^2}. \tag{31}$$

Each point of the line moves on a rail with a disordered potential that is uncorrelated with the other rails, so that $\Delta_x(x - x') = \delta_{x,x'}$. Three different models of disorder are considered:

- model A: random field disorder obtained by the linear interpolation of the random force drawn at the extremities of segments of length 1;
- model B: random field disorder obtained in the same way as model A, but the segments have length 0.1 with probability 1/2 and 1.9 with probability 1/2;
- model C: random bond disorder obtained by the spline interpolation of the random energies drawn at the extremities of segments of length 1.

J. Stat. Mech. (2014) P03009

5.2. Analytical prediction

A prediction of the critical force for the three models can be obtained by observing that for a discrete line the damping rate (18) changes to

$$\omega(k_x) = \kappa + c\left(|k_x| - \frac{ak_x^2}{2\pi}\right), \tag{32}$$

where the wavevector k_x is restricted to $[-\pi/a, \pi/a]$. The limits $\kappa \to 0$ and $v \to 0$ give exactly the same result as (8),

$$f_{c,2} = \lim_{v\to 0}\lim_{\kappa\to 0} f_{\mathrm{tot},2}(v,\kappa) = \frac{\sigma^2\tilde{\Delta}_x(0)}{4\pi c}\int |k_u|\tilde{\Delta}_u(k_u)\,\mathrm{d}k_u. \tag{33}$$

It is remarkable that discretizing the line does not change the critical force. In all models we set $a = 1$ so that $\tilde{\Delta}_x(0) = 1$ and the functional of $\Delta_u(u)$ appearing in our expression (8) for the critical force is computed in appendix A for the three models. The final prediction for model A is

$$f_{c,2} = \frac{2\log(2)}{\pi}\frac{\sigma^2}{c} \simeq 0.44\frac{\sigma^2}{c}, \tag{34}$$

while for model B a numerical computation gives

$$f_{c,2} \simeq 0.55\frac{\sigma^2}{c}, \tag{35}$$

and for model C we have

$$f_{c,2} \simeq 2.83\frac{\sigma^2}{c}. \tag{36}$$

5.3. Measurement of the critical force

We start our numerical procedure with a flat configuration $u(x) = 0$ and $w = 0$. Then the interface moves to a state $u_{w=0}(x)$ that is stable with respect to small deformations. Increasing w, the interface position increases and a sequence of stable states can be recorded. For each w, the stable state $u_w(x)$ can be found using the algorithm proposed in [34] and we measure the pinning force

$$f_w(\kappa) = \kappa[w - \langle u_w(x)\rangle]. \tag{37}$$

This pinning force depends on the realization of the disordered potential (its fluctuations have been studied in [35]). An example of the evolution of the pinning force with w is shown in figure 4. The pinning force is in general dependent on the initial condition; however, due to the Middleton no-passing rule [36], we can prove that there exists a $w^* > 0$ such that the sequence of stable states $u_{w>w^*}(x)$ becomes independent of the initial condition. A stationary state is thus reached, where the pinning force oscillates around its average value $\overline{f(\kappa)}$ and displays correlation in w. Thus, in order to estimate $\overline{f(\kappa)}$ correctly we sample $f_w(\kappa)$ far enough from the origin $w = 0$ and for values of w far enough from each other.

J. Stat. Mech. (2014) P03009

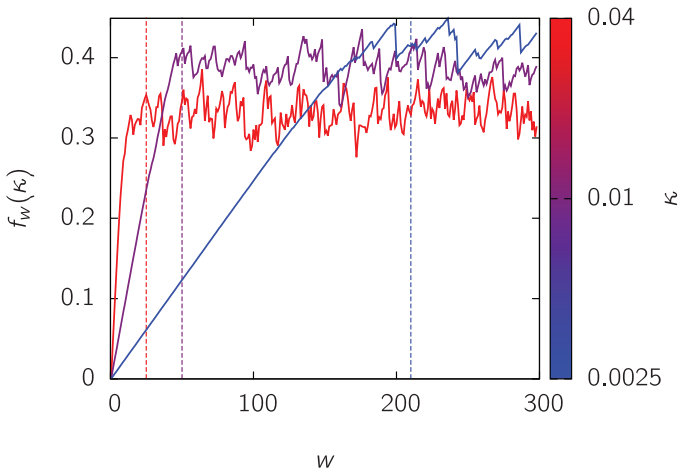

Figure 4. The pinning force (37) as a function of the position w of the parabola, for different values of the spring stiffness κ. The dashed vertical lines represent approximate values w^* after which the pinning force becomes independent of the initial condition. Model A disorder with $\sigma = 1$ is used here.

An exact relation (the statistical tilt symmetry [37]) assures that the quadratic part of the Hamiltonian (and thus the constant κ) is not renormalized. This means that the length associated by a simple dimensional analysis to the bare constant κ, namely $L_\kappa = c/\kappa$, corresponds to the correlation length of the system: above L_κ the interface is flat and feels the harmonic parabola only, while below L_κ the interface is rough with the characteristic roughness exponent at depinning $\zeta \simeq 0.39$ [34].

The separation from the critical depinning point (located exactly at the critical driving force f_c) is described by the power law scaling [38] $f - f_c \sim \xi^{-1/\nu}$, where ξ is the correlation length, given in our case by L_κ. When $\kappa \to 0$ (while keeping $L \gg L_\kappa$), the pinning force tends to the thermodynamical critical force f_c. Gathering the previous scalings, we thus have that the finite size effects on the force take the form

$$\overline{f(\kappa)} = f_c + c_1 \kappa^{1/\nu} + \cdots . \tag{38}$$

The fluctuations around this value, $\overline{\delta f(\kappa)^2}$, depend on L and κ. In the limit $L \gg L_\kappa = 1/\kappa$, the interface can be modelled as a collection of independent interfaces of size L_κ and the central limit theorem assures that the variance $\overline{\delta f(\kappa)^2}$ should scale as $\sim \kappa^{2/\nu}$, but with an extra factor L_κ/L. This allows us to write an extrapolation formula for f_c that is independent of the critical exponent ν,

$$\overline{f(\kappa)} = f_c + c_1 \sqrt{\kappa L \overline{\delta f(\kappa)^2}} + \cdots . \tag{39}$$

Our determination of f_c is performed using this relation, by extrapolating the numerical measurements of $\overline{f(\kappa)}$ for different values of κ to the limit $\kappa \to 0$, as shown in figure 5. It is worth noticing that most of the details of the finite size system such as the boundary conditions or the presence of the parabolic well do not affect the thermodynamic value of f_c, which depends only on the elastic constant c and on the disorder statistics

J. Stat. Mech. (2014) P03009

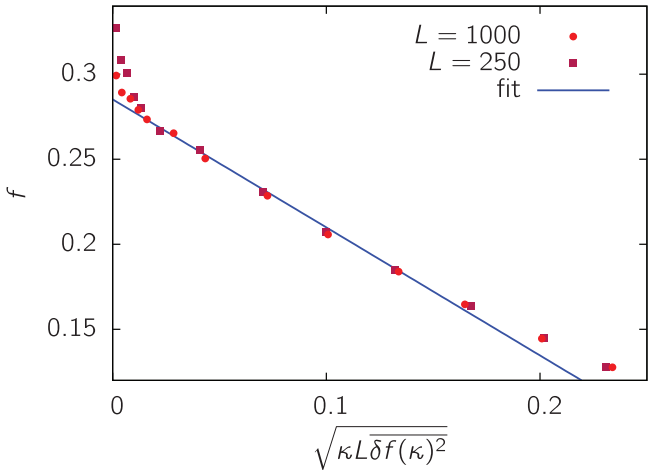

Figure 5. The pinning force averaged over the parabola position w, versus a function of the spring stiffness. A fit of the linear part gives the critical force, see equation (39). This plot is for model A disorder with $\sigma = 0.8$ and we found $f_c = 0.285$.

[39, 40]. Our extrapolation of f_c, shown in figure 5, has been performed on samples of size $L = 1000, 4000$ (depending on the value of sigma) and for parabola curvatures down to $\kappa = 10^{-4}$.

5.4. Results

The dimensionless critical force $F_c = f_c/\sigma$ is plotted versus the dimensionless disorder parameter

$$\Sigma = \frac{\sigma \tilde{\Delta}_x(0)}{4\pi c} \int |k_u| \tilde{\Delta}_u(k_u)\, \mathrm{d}k_u \tag{40}$$

in figure 2. In all three cases, the results are very close to the theoretical prediction $F_c = \Sigma$ (equivalent to equation (8)) when the disorder parameter is small.

6. Conclusion

We have shown that the critical force for a long-range elastic line in a random landscape can be computed perturbatively in the collective pinning regime, yielding the expression (8). Our result for the critical force gives, together with its scaling with respect to the microscopic parameters, its dependence on the disorder geometry. Indeed, we have shown that two disorders that can be attributed the same correlation lengths (as in models A and B) may present different critical forces that are precisely predicted by our theory.

Some previous works have studied the scaling of the critical force with respect to microscopic parameters such as the disorder amplitude σ, the elastic constant c and the disorder correlation lengths ξ_x and ξ_u in the directions x and u [5, 24, 27]. In particular,

J. Stat. Mech. (2014) P03009

for the long-range elastic line, the following scaling has been found for the critical force in the collective pinning regime [27]:

$$f_c \sim \frac{\sigma^2 \xi_x}{c \xi_u}. \tag{41}$$

The lengths ξ_x and ξ_u characterize the typical scale of the disorder correlation along x and u, but these scales cannot be uniquely defined. Different definitions lead to correlation lengths that differ only by a numerical factor, so the scaling law (41) holds independently of the chosen definitions. However, this prevents the use of this scaling law to make a quantitative prediction. Our formula allows us to overcome this problem. In particular, starting from equation (8) and writing

$$\Delta_x(x) = \Delta_{x1}(x/\xi_x), \tag{42}$$

where Δ_{x1} is a function of the dimensionless variable x/ξ_x and a similar relation defines Δ_{u1}, one gets

$$f_c = \left(\frac{\tilde{\Delta}_{x1}(0)}{4\pi} \int |q_u| \tilde{\Delta}_{u1}(q_u)\, \mathrm{d}q_u \right) \times \frac{\sigma^2 \xi_x}{c \xi_u}. \tag{43}$$

This shows that our analytical prediction (8) allows us to recover the scaling law (41) and gives additionally the prefactor as a function of the correlation functions, i.e. it yields the explicit dependence of the critical force on the disorder geometry.

The present work is not the first attempt to compute the critical force perturbatively: expansions have been performed at weak disorder [18, 41], low temperature [31] or large velocity [42, 43]. Weak disorder expansions are valid up to the Larkin length [5], L_c, defined as the distance at which the line wanders enough to see the finite disorder correlation length ξ_u (namely $|u(L_c) - u(0)| \simeq \xi_u$). Above the Larkin length, however, they predict an incorrect roughness exponent [44]. Lastly, large velocity expansions give an estimation of the critical force that is obtained by continuing a large-velocity asymptotic result, which lies very far from the depinning regime, to zero velocity. Our computation does not need such continuation, and is compatible with the fact that perturbative expansions in the disorder amplitude are incorrect above the Larkin length, since the critical force can be evaluated from the line behaviour at the scale of the Larkin length [5].

Our analysis is a first step towards a more general understanding of the critical force dependence, and it can be extended in several directions. Firstly, the opposite *individual* pinning regime occurring at a high disorder amplitude is worthy of investigation. The perturbative analysis used here is not suited for its study, but a few comments can be made on the grounds of former numerical studies [27, 28]. Its scaling with respect to the disorder amplitude and correlation length has been elucidated for a long-range elastic line, giving [27]

$$f_c \sim \sigma; \tag{44}$$

thus the critical force is now proportional to the disorder amplitude and does not depend on the disorder correlation lengths. Moreover, we have shown in a previous study [27] that the critical force is given by the strongest pinning sites if the pinning force is bounded.

J. Stat. Mech. (2014) P03009

In this case, it is likely that the dependence on the disorder geometry is very weak. The case of unbounded pinning force requires further investigation.

Another issue arising from our study is the question of the landscape smoothness. Our analysis requires an expansion of the potential to second order around the position of the unperturbed line (see equation (20)): the force generated by the potential must be continuous. When one tries to apply the analytical prediction (8) to a discontinuous force landscape, it diverges because of a cusp present in the correlation function $\Delta_u(u)$. On the other hand, our previous numerical study [27] used a discontinuous force landscape and did not reveal any divergence, while the dependence on the disorder amplitude, $f_c \sim \sigma^2$, was the same as the one observed here. This suggests that the divergence obtained when we try to apply our result to a discontinuous force landscape is regularized by a mechanism that is out of reach of the present perturbative computation. An understanding of the behaviour of the elastic line and the critical force in a rougher force landscape would be an important advance from a theoretical point of view, but also for experiments where discontinuous force landscapes are ubiquitous [8, 11].

Lastly, the case of a short-range instead of long-range elasticity remains to be understood within our approach; interesting comparison could be established with the characteristic force of the creep regime, whose dependence on the details of the disorder correlator (for RB disorder) has been examined recently [45]–[47].

Acknowledgments

We would like to thank L Ponson and E Agoritsas for fruitful discussions and for a critical reading of the manuscript. VD acknowledges support from the Institut des Systèmes Complexes de Paris Île de France.

Appendix. Disorder generation and correlation

We detail here the procedures used to generate the different models of disorder, and how to compute the disorder correlation function, which is needed to evaluate the critical force (8).

A.1. Random field disorder: models A and B

For a random field disorder, the disorder is generated on each rail using the following procedure (see figure A.1).

- The rail is divided into segments of random length l drawn in the distribution $P(l)$.
- At the point linking the segment $j-1$ and the segment j, a random force f_j is drawn from a Gaussian distribution with zero mean and unit variance.
- Inside the segment j, at a generic point u, the force $f(u)$ is obtained by a linear interpolation such that $f(u_j) = f_j$ and $f(u_{j+1}) = f_{j+1}$.

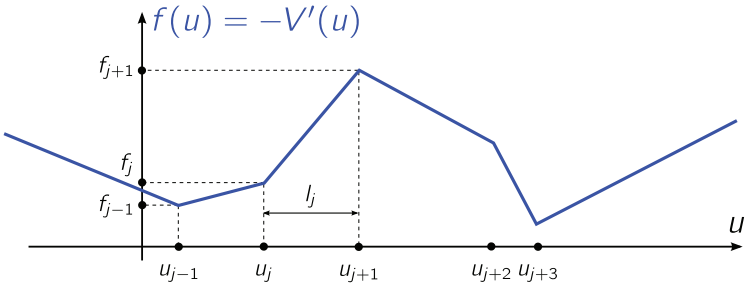

Figure A.1. Random field disorder on a rail: the force is continuous and piecewise linear.

We want to know the correlation of the forces at two points separated by a distance $u \geq 0$, say $f(0)$ and $f(u)$. This correlation is non-zero if the two points lie on the same segment or on neighbouring segments. We introduce the length l of the segment where the point 0 lies, the length l' of its right neighbour, and the left end u_0 of the first segment. The probability distribution for l is $Q(l) = lP(l)/\bar{l}$, where $\bar{l} = \int_0^\infty P(l)\,\mathrm{d}l$; the probability distribution for l' is simply $P(l')$ and the one of u_0 is $l^{-1}\chi_{[-l,0]}(u_0)$ (meaning that the point 0 is uniformly distributed in its segment). Putting these probabilities together, we get the probability distribution for (l, l', u_0),

$$\mathbb{P}(l, l', u_0) = \bar{l}^{-1} P(l) P(l') \chi_{[-l,0]}(u_0). \tag{A.1}$$

The points 0 and u are on the same segment if $u \leq u_0 + l$. The force at u_0 is f_0 and the force at $u_0 + l$ is f_1; f_0 and f_1 are uncorrelated random variables with zero mean and unit variance. The forces at 0 and u are

$$f(0) = f_0 \frac{u_0 + l}{l} + f_1 \frac{-u_0}{l}, \tag{A.2}$$

$$f(u) = f_0 \frac{u_0 + l - u}{l} + f_1 \frac{u - u_0}{l}. \tag{A.3}$$

The correlation between these two forces is

$$\overline{f(0)f(u)} = \frac{2u_0^2 + 2(l-u)u_0 + l^2}{l^2}. \tag{A.4}$$

Here, the average is restricted to the forces f_0 and f_1; the other variables l, l' and u_0 are fixed. On the other hand, when $u_0 + l \leq u \leq u_0 + l + l'$, the two points lie on neighbouring segments. The same argument gives for the force correlation

$$\overline{f(0)f(u)} = \frac{-u_0^2 - (l + l' - u)u_0}{ll'}. \tag{A.5}$$

J. Stat. Mech. (2014) P03009

Gathering the results (A.1), (A.4) and (A.5) and integrating over u_0 gives for the correlation function

$$\Delta_u(u) = \frac{1}{\bar{l}} \int_0^\infty \mathrm{d}l\, P(l) \left(\chi_{[0,l]}(u) \frac{u^3 - 3l^2 u + 2l^3}{3l^2} + \int_0^\infty \mathrm{d}l' P(l') \chi_{[0,l+l']}(u) \left[\frac{-2u_0^3 - 3(l+l'-u)u_0^2}{6ll'} \right]_{\max(u-l-l',-l)}^{\min(u-l,0)} \right), \tag{A.6}$$

where we have used the notation $[g(u_0)]_a^b = g(b) - g(a)$.

For the model A, all the segments have the same length $l = 1$, corresponding to the probability density

$$P(l) = \delta(l-1). \tag{A.7}$$

For the model B, the segment lengths can take two values, 0.1 and 1.9, with probability 1/2 each,

$$P(l) = \tfrac{1}{2}\delta(l-0.1) + \tfrac{1}{2}\delta(l-1.9). \tag{A.8}$$

For the model A, inserting the probability density (A.7) into the general formula (A.6) gives the correlation function for $u \geq 0$,

$$\Delta_u(u) = \chi_{[0,1]}(u) \frac{3u^3 - 6u^2 + 4}{6} + \chi_{(1,2]}(u) \frac{(2-u)^3}{6}. \tag{A.9}$$

It is plotted in figure A.2. To compute the critical force (8), we need the following quantity:

$$\int |k_u| \tilde{\Delta}_u(k_u)\, \mathrm{d}k_u = 4 \int_0^\infty \frac{\Delta_u(0) - \Delta_u(u)}{u^2}\, \mathrm{d}u = 8 \log(2). \tag{A.10}$$

For the model B, the correlation function is more complex and is plotted in figure A.2. The integral entering the expression (8) of the critical force has to be computed numerically; we get

$$\int |k_u| \tilde{\Delta}_u(k_u)\, \mathrm{d}k_u \simeq 6.91. \tag{A.11}$$

A.2. Random bond disorder: model C

A random bond disorder can be generated on a rail by drawing random energies for points on a grid of step l. A spline interpolation of these energies then allows one to get a smooth landscape of potential. We determine here the two-point correlation function of such a disorder (see [47] for a similar study for a two-dimensional spline). Specifically, let us consider a grid of spacing l with $2n+1$ points indexed from $-n$ to n. A random value V_i is attached to each site $u_i = il$ of the grid. The function $V(u)$ is a cubic spline of the $(V_i)_{-n \leq i \leq n}$, that is

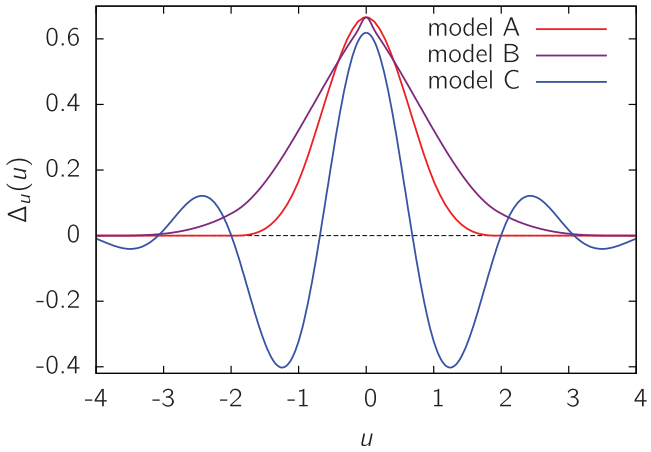

Figure A.2. The two-point correlation function of the force $\Delta_u(u) = \overline{\partial_u V(0)\partial_u V(u)}$ for the disorder models A, B and C. The model C correlation function has been rescaled by a factor of 0.25.

- $V(u)$ is a cubic polynomial on each lattice segment $[u_i, u_{i+1}]$ for $-n \leq i < n$,
- $V(u)$ is continuous on each lattice site u_i, and equal to V_i, $V(u_i^+) = V(u_i^-) = V_i$,
- the first and second derivatives of $V(u)$ are continuous, $V'(u_i^+) = V'(u_i^-)$ and $V''(u_i^+) = V''(u_i^-)$.

One defines the coefficients $A_i^0, \ldots, A_i^3$ $(-n \leq i < n)$ of the polynomials as

$$V(u) = A_i^0 + A_i^1(u - u_i) + \frac{A_i^2}{2}(u - u_i)^2 + \frac{A_i^3}{3!}(u - u_i)^3 \tag{A.12}$$

for $u_i \leq u < u_{i+1}$. One has $A_i^0 = V_i$.

Denoting $l_i = u_{i+1} - u_i$ (it does not need to be constant, we will keep it generic for a while), the continuity conditions are written as

$$A_{i+1}^0 = A_i^0 + l_i A_i^1 + \frac{1}{2} l_i^2 A_i^2 + \frac{1}{3!} l_i^3 A_i^3, \tag{A.13}$$

$$A_{i+1}^1 = A_i^1 + l_i A_i^2 + \tfrac{1}{2} l_i^2 A_i^3, \tag{A.14}$$

$$A_{i+1}^2 = A_i^2 + l_i A_i^3. \tag{A.15}$$

There are $6n$ unknown variables and $6n - 2$ bulk equations (A.13)–(A.15). They have to be complemented by boundary conditions (e.g. fixing the values of the derivatives at extremities, or imposing periodic boundary conditions). The simplest way to solve the set of equations is to eliminate the A_i^1 s and the A_i^3 s to obtain equations on the A_i^2 s only, as a function of the parameters l_i and $A_i^0 = V_i$. From (A.15) one has $A_i^3 = (A_{i+1}^2 - A_i^2)/l_i$ and substituting into (A.13) one obtains A_i^1,

$$A_i^1 = \frac{A_{i+1}^0 - A_i^0}{l_i} - l_i \frac{2A_i^2 + A_{i+1}^2}{6}. \tag{A.16}$$

Using these expressions in (A.14) one gets the equations on the A_i^2 s,

$$l_i A_i^2 + 2(l_i + l_{i+1})A_{i+1}^2 + l_{i+1}A_{i+2}^2 = 6\frac{A_{i+2}^0 - A_{i+1}^0}{l_{i+1}} - 6\frac{A_{i+1}^0 - A_i^0}{l_i}. \tag{A.17}$$

These are quite complex to solve in general but simplifications occur for an uniform spacing $l_i = l$ and in the infinite grid size limit $n \to \infty$.

Solution for constant $l_i = l$: the equations are written as

$$A_i^2 + 4A_{i+1}^2 + A_{i+2}^2 = \frac{6}{h^2}(A_i^0 - 2A_{i+1}^0 + A_{i+2}^0). \tag{A.18}$$

They take the form $M\vec{A^2} = (6/h^2)\Delta\vec{A^0}$, where Δ is the discrete Laplacian and M is a tridiagonal $(2n+1)\times(2n+1)$ matrix. It is best represented as $M = 6(\mathbf{1} + \Delta/6)$ with

$$\Delta = \begin{pmatrix} -2 & 1 & 0 & 0 & \dots \\ 1 & -2 & 1 & 0 & \dots \\ 0 & 1 & -2 & 1 & \\ \vdots & & \ddots & \ddots & \ddots \end{pmatrix}, \tag{A.19}$$

which allows us to invert M by writing

$$M^{-1} = \frac{1}{6}\sum_{p\geq 0}\frac{(-1)^p}{6^p}\Delta^p. \tag{A.20}$$

Hence, the vector $\vec{A^2}$ of the A_i^2 s is obtained as

$$\vec{A^2} = \frac{1}{l^2}\sum_{p\geq 0}\frac{(-1)^p}{6^p}\Delta^{p+1}\vec{A^0}. \tag{A.21}$$

Each of the A_i^2 s is a linear combination of all the fixed potentials $A_i^0 = V_i$. It is known that the coefficients of Δ^p are given in the infinite size limit $n \to \infty$ by the binomial coefficients, up to a sign. For instance, the diagonal and subdiagonal elements are

$$(\Delta^p)_{ii} = (-1)^p\binom{2p}{p}, \qquad (\Delta^p)_{i,i+1} = (-1)^{p+1}\binom{2p}{p-1}. \tag{A.22}$$

One is now ready to determine the correlator of the potential. On a generic interval $il \leq y \leq (i+1)l$ $(i > 0)$ one has

$$V(u+\eta) = \left(i + 1 - \frac{u}{l}\right)A_i^0 - \left(i - \frac{u}{l}\right)A_{i+1}^0 + \frac{(u-il)(u-(i+1)l)}{6l} \times \left[((2+i)l - u)A_i^2 + (u - (i-1)l)A_{i+1}^2\right], \tag{A.23}$$

where η is uniformly distributed on $[0, l]$ and allows one to implement the statistical invariance by translation of the disorder (and generalizes the result of [47]). To determine the correlation function $\overline{V(u)V(u')}$, one thus has to identify the segments to which u and

u' belong, and, expanding (A.23), to determine averages of the form $\overline{A_i^0 A_j^2}$. These are obtained from the large-n limit explicit form of (A.21), which reads

$$\begin{aligned} A_j^2 &= \cdots + (-1)^i \frac{1}{l^2} \sum_{p\geq 0} \frac{1}{6^p} \binom{2p+2}{p-i+1} A_{j+i}^0 + \cdots \\ &= \cdots + (-1)^{i+1} \frac{6\sqrt{3}}{l^2} \left(2-\sqrt{3}\right)^i A_{j+i}^0 + \cdots , \end{aligned} \tag{A.24}$$

which yields for instance $\overline{A_0^0 A_i^2} = (-1)^{i+1} 6\sqrt{3}/l^2 (2-\sqrt{3})^i$. One obtains a cumbersome expression in real space, defined piecewise, which we do not reproduce here for clarity. After Fourier transformation, the correlator $\tilde{R}_u$ is found to take a simple form

$$\tilde{R}_u(k_u) = \frac{9 \sin(k_u/2)^8}{(2+\cos(k_u))^2}, \tag{A.25}$$

which we have checked numerically. The force correlation function is shown in figure A.2; unlike the random field correlation functions, it presents negative parts indicating anticorrelations of the disorder (due to the spline continuity constraints).

References

[1] Halpin-Healy T and Zhang Y-C, *Kinetic roughening phenomena, stochastic growth, directed polymers and all that*, 1995 *Phys. Rep.* **254** 215
[2] Kardar M, *Nonequilibrium dynamics of interfaces and lines*, 1998 *Phys. Rep.* **301** 85–112
[3] Brazovskii S and Nattermann T, *Pinning and sliding of driven elastic systems: from domain walls to charge density waves*, 2004 *Adv. Phys.* **53** 177–252
[4] Agoritsas E, Lecomte V and Giamarchi T, *Disordered elastic systems and one-dimensional interfaces*, 2012 *Physica* B **407** 1725–33
[5] Larkin A I and Ovchinnikov Y N, *Pinning in type II superconductors*, 1979 *J. Low Temp. Phys.* **34** 409–28
[6] Lemerle S, Ferré J, Chappert C, Mathet V, Giamarchi T and Le Doussal P, *Domain wall creep in an ising ultrathin magnetic film*, 1998 *Phys. Rev. Lett.* **80** 849–52
[7] Joanny J F and de Gennes P G, *A model for contact angle hysteresis*, 1984 *J. Chem. Phys.* **81** 552–62
[8] Soriano J, Ortín J and Hernández-Machado A, *Experiments of interfacial roughening in Hele-Shaw flows with weak quenched disorder*, 2002 *Phys. Rev.* E **66** 031603
[9] Santucci S, Planet R, Jørgen Måløy K and Ortín J, *Avalanches of imbibition fronts: towards critical pinning*, 2011 *Europhys. Lett.* **94** 46005
[10] Bouchaud E, Bouchaud J P, Fisher D S, Ramanathan S and Rice J R, *Can crack front waves explain the roughness of cracks?*, 2002 *J. Mech. Phys. Solids* **50** 1703–25
[11] Bonamy D, Santucci S and Ponson L, *Crackling dynamics in material failure as the signature of a self-organized dynamic phase transition*, 2008 *Phys. Rev. Lett.* **101** 045501
[12] Barabási A-L and Stanley H E, 1995 *Fractal Concepts in Surface Growth* (Cambridge: Cambridge University Press)
[13] Krug J, *Origins of scale invariance in growth processes*, 1997 *Adv. Phys.* **46** 139–282
[14] Bustingorry S, Kolton A B and Giamarchi T, *Thermal rounding of the depinning transition*, 2008 *Europhys. Lett.* **81** 26005
[15] Ioffe L B and Vinokur V M, *Dynamics of interfaces and dislocations in disordered media*, 1987 *J. Phys.* C: *Solid State Phys.* **20** 6149
[16] Nattermann T, *Scaling approach to pinning: Charge density waves and giant flux creep in superconductors*, 1990 *Phys. Rev. Lett.* **64** 2454
[17] Balents L and Fisher D S, *Large-n expansion of $(4-\varepsilon)$-dimensional oriented manifolds in random media*, 1993 *Phys. Rev.* B **48** 5949–63
[18] Chauve P, Giamarchi T and Le Doussal P, *Creep and depinning in disordered media*, 2000 *Phys. Rev.* B **62** 6241–67

J. Stat. Mech. (2014) P03009

[19] Kolton A B, Rosso A, Giamarchi T and Krauth W, *Creep dynamics of elastic manifolds via exact transition pathways*, 2009 *Phys. Rev.* B **79** 184207

[20] Anderson P W and Kim Y B, *Hard superconductivity: theory of the motion of abrikosov flux lines*, 1964 *Rev. Mod. Phys.* **36** 39–43

[21] Chauve P, Le Doussal P and Jörg Wiese K, *Renormalization of pinned elastic systems: how does it work beyond one loop?*, 2001 *Phys. Rev. Lett.* **86** 1785–8

[22] Le Doussal P, Jörg Wiese K and Chauve P, *Functional renormalization group and the field theory of disordered elastic systems*, 2004 *Phys. Rev.* E **69** 026112

[23] Joerg Wiese K and Doussal P L, *Functional renormalization for disordered systems, basic recipes and gourmet dishes*, 2007 *Markov Processes, Relat. Fields* **13** 777 [arXiv:cond-mat/0611346]

[24] Nattermann T, Shapir Y and Vilfan I, *Interface pinning and dynamics in random systems*, 1990 *Phys. Rev.* B **42** 8577–86

[25] Roux S, Vandembroucq D and Hild F, *Effective toughness of heterogeneous brittle materials*, 2003 *Eur. J. Mech.* A **22** 743–9

[26] Roux S and Hild F, *Self-consistent scheme for toughness homogenization*, 2008 *Int. J. Fract.* **154** 159

[27] Démery V, Ponson L and Rosso A, From microstructural features to effective toughness in disordered brittle solids, 2012 arXiv:1212.1551

[28] Patinet S, Vandembroucq D and Roux S, *Quantitative prediction of effective toughness at random heterogeneous interfaces*, 2013 *Phys. Rev. Lett.* **110** 165507

[29] Ferrero E E, Bustingorry S, Kolton A B and Rosso A, *Numerical approaches on driven elastic interfaces in random media*, 2013 *C. R. Phys.* **14** 641–50

[30] Larkin A I, *Effect of inhomogeneities on the structure of the mixed state of superconductors*, 1970 *Sov. Phys.—JETP* **31** 784

[31] Chen L-W and Cristina Marchetti M, *Interface motion in random media at finite temperature*, 1995 *Phys. Rev.* B **51** 6296–308

[32] Fisher D S, *Collective transport in random media: from superconductors to earthquakes*, 1998 *Phys. Rep.* **301** 113–50

[33] Duemmer O and Krauth W, *Depinning exponents of the driven long-range elastic string*, 2007 *J. Stat. Mech.* **2007** P01019

[34] Rosso A and Krauth W, *Roughness at the depinning threshold for a long-range elastic string*, 2002 *Phys. Rev.* E **65** 025101

[35] Bolech C J and Rosso A, *Universal statistics of the critical depinning force of elastic systems in random media*, 2004 *Phys. Rev. Lett.* **93** 125701

[36] Alan Middleton A, *Asymptotic uniqueness of the sliding state for charge-density waves*, 1992 *Phys. Rev. Lett.* **68** 670–3

[37] Schulz U, Villain J, Brézin E and Orland H, *Thermal fluctuations in some random field models*, 1988 *J. Stat. Phys.* **51** 1–27

[38] Nattermann T, Stepanow S, Tang L-H and Leschhorn H, *Dynamics of interface depinning in a disordered medium*, 1992 *J. Physique* II **2** 1483–8

[39] Kolton A B, Bustingorry S, Ferrero E E and Rosso A, *Uniqueness of the thermodynamic limit for driven disordered elastic interfaces*, 2013 *J. Stat. Mech.* P12004

[40] Budrikis Z and Zapperi S, *Size effects in dislocation depinning models for plastic yield*, 2013 *J. Stat. Mech.* P04029

[41] Efetov K B and Larkin A I, *Charge-density wave in a random potential*, 1977 *Sov. Phys.—JETP* **45** 1236–41

[42] Schmid A and Hauger W, *On the theory of vortex motion in an inhomogeneous superconducting film*, 1973 *J. Low Temp. Phys.* **11** 667–85

[43] Larkin A I and Ovchinnikov Y N, *Electrodynamics of inhomogeneous type-II superconductor*, 1974 *JETP* **38** 854

[44] Kardar M, *Replica Bethe ansatz studies of two-dimensional interfaces with quenched random impurities*, 1987 *Nucl. Phys.* B **290** 582–602

[45] Agoritsas E, Lecomte V and Giamarchi T, *Temperature-induced crossovers in the static roughness of a one-dimensional interface*, 2010 *Phys. Rev.* B **82** 184207

[46] Agoritsas E, Lecomte V and Giamarchi T, *Static fluctuations of a thick one-dimensional interface in the* $1+1$ *directed polymer formulation*, 2013 *Phys. Rev.* E **87** 042406

[47] Agoritsas E, Lecomte V and Giamarchi T, *Static fluctuations of a thick one-dimensional interface in the* $1+1$ *directed polymer formulation: numerical study*, 2013 *Phys. Rev.* E **87** 062405

J. Stat. Mech. (2014) P03009